Neutron diffraction study of the nuclear and magnetic structure of the quasi-one-dimensional compound $CuSiO_3$ around $T_N = 8$ K

H. Wolfram and H. H. Otto
Fachgebiet Materialwissenschaftliche Kristallographie, TU Clausthal, Adolph-Roemer-Straße 2A, D-38678 Clausthal-Zellerfeld, Germany

M. Cwik and M. Braden
II. Physikalisches Institut, Universität Köln, Zülpicher Straße 77, D-50937 Köln, Germany

G. André and F. Bourée
Laboratoire Léon Brillouin, CEA, CNRS, CE-Saclay, 91191 Gif sur Yvette Cedex, France

M. Baenitz and F. Steglich
Max-Planck-Institute of Chemical Physics of Solids, D-01187 Dresden, Germany

(Received 25 July 2003; revised manuscript received 3 December 2003; published 21 April 2004)

We investigated the nuclear and magnetic structure of $CuSiO_3$ by neutron powder diffraction methods at room temperature and around $T_N = 8$ K. With decreasing temperature the lattice parameters showed, similar to $CuGeO_3$, decreasing *a* and *b* parameters and a slightly increasing *c* parameter down the chain direction. Below the second order phase transition at T_N we observed for $CuSiO_3$ the appearance of a small set of magnetic superstructure reflections; the determined antiferromagnetic order can be described by a commensurate propagation vector of $\mathbf{q} = (1/2, 0, 1/8)$ with respect to the chemical *Pbmm* unit cell. From the long modulation along the chain a ferromagnetic next neighbor magnetic exchange is deduced, whereas next nearest neighbor coupling is expected to be antiferromagnetic.

DOI: 10.1103/PhysRevB.69.144115 PACS number(s): 61.12.−q, 75.50.Ee

I. INTRODUCTION

Low-dimensional quantum spin systems are of considerable theoretical and experimental interest together with some applications to which they may lead. Copper polygermanate $CuGeO_3$ with its rather simple crystal structure of single chains of GeO_4 tetrahedra and $S = 1/2$ spin chains of edge-sharing CuO_{4+2} octahedra,[1,2] is the unique inorganic compound showing the spin-Peierls transition.[3,4] In this compound neighboring antiferromagnetic Heisenberg chains exhibit a spin dimerization at $T_{sp} = 14.3$ K resulting in an exponentially vanishing magnetic susceptibility in all crystallographic directions with decreasing temperature; the Cu^{2+} spins condense into a nonmagnetic spin-singlet ground state. A small shift of the atomic positions, which mediates the superexchange in the magnetic chains, accompanies this magnetic dimerisation. The space group transforms below T_{sp} from *Pbmm* into *Bbcm* with a doubling of the *a* and *c* lattice parameters. As a quasi-one-dimensional system with unique properties $CuGeO_3$ has been the subject of intensive experimental and theoretical work in the past years. Fortunately, the very stable crystal structure is receptive to partial ionic substitutions and the influence of doping effects on its thermodynamic and magnetic properties could be systematically investigated.[5–9] For instance, the substitution of Ge by Si according to $CuGe_{1-x}Si_xO_3$ was possible up to $x \leqslant 50$ atomic percent.[10] Even a minute Si concentration causes first a reduction and finally a suppression of the spin-Peierls transition and induces a Néel state ($T_N < T_{sp}$).[5–7,9] This impurity-induced magnetic state can coexist with the singlet ground state.[8] The complexity of impurity-induced ordered phases in low-dimensional spin-gap systems was recently reviewed by Uchinokura.[11] Also a magnetic field induced transition from the spin-Peierls state into an incommensurate spin-lattice modulated phase forming a soliton lattice has been observed.[12] Pure $CuSiO_3$, on the other hand, was considered nonexistent in the past.[13] It was therefore a great surprise when Otto and Meibohm[14] succeeded in the synthesis of the pure copper polysilicate by thermal decomposition of the mineral dioptase $Cu_6Si_6O_{18} \cdot 6H_2O$. Dioptase was proposed to exhibit a quantum phase transition between an antiferromagnetically ordered state and a quantum spin liquid.[15] At room temperature $CuSiO_3$ is isotypic to the $CuGeO_3$ prototype. Copper polysilicate, however, does not show the spin-Peierls effect, instead we will show that it exhibits a long-range antiferromagnetic ordering below 8 K.[16] The compound has lattice parameters, which are changed in a remarkable way in comparison with $CuGeO_3$: *a* and *c* are reduced by about 3.5 and 3.7 %, respectively, whereas *b* is enlarged by about 3.5%. As a consequence of the reduced chain periodicity *c* the bond valence contribution of the O(2) atoms to copper is increased. This increase has to be compensated for by a larger separation of the O(1) atoms of the copper surrounding leading to the very large Jahn-Teller distortion observed, the CuO_{4+2} ''octahedral'' chains are degenerated to CuO_2 ribbons. The changed atomic distances cause a rotation of these chains in the *ab* plane of $\Delta\tau \approx 10°$, shortening the *a* axis and enlarging the *b* axis of $CuSiO_3$ in comparison to $CuGeO_3$. In this way the CuO_2 ribbons have a larger separation from each other in the *b* direction being $b/2 = 4.39$ Å for the silicate compared to 4.23 Å for the germanate. The *ac* layerlike character of the germanate as a consequence of its large chain separation in the

a direction, corresponding to the lattice parameter $a = 4.80$ Å, turns over into a more three-dimensional (3D) behavior of the silicate with only $a = 4.63$ Å. A case in point is that for the silicate the O(2)-Cu-O(2) angle is about $\eta = 95°$ and nearer to 90° than the corresponding 99° angle for the germanate; this angle is considered to be important, besides the strength of the crystal field, for the different magnetic interaction and ground state properties found for both compounds.

We notice that very recently another compound, the copper arsenate hydroxide mineral theoparacelsite $CuAs_{2/3}H_{2/3}O_3$ was identified to be isotypic to the two compounds mentioned above. This phase shows disrupted arsenate single chains, because one third of the As positions are vacant.[17]

Comparing further properties of $CuGeO_3$ and $CuSiO_3$ we are faced with the very different color of the two compounds. Whereas $CuGeO_3$ is light greenish blue, the color of the mixture, consisting of the main phase $CuSiO_3$ in addition to minor phases CuO (tenorite) and SiO_2 (amorphous), is very rich brownish black and definitely darker than pure CuO. Therefore, absorption bands of the optical spectrum for $CuSiO_3$ are tailing off into the blue end of the visible spectrum.

It was the objective of the present study to complete the various experiments already done on $CuSiO_3$, such as x-ray diffraction,[14] measurements of magnetization, specific heat, ^{63}Cu-NQR and ESR,[16,18] as well as Raman and IR spectroscopic studies[19] with neutron diffraction investigations at low temperature as an essential tool to probe phase transitions and related critical phenomena. Here we present results of the nuclear and magnetic structure of $CuSiO_3$ derived from neutron scattering investigations at room temperature and around $T_N = 8$ K and compare the conclusions with those given for the isotypic compound $CuGeO_3$.[2,20–22]

II. EXPERIMENTAL DETAILS

About 1 cm^3 of a multiphase sample containing around 72 wt. % of $CuSiO_3$, 16 wt. % CuO (tenorite) and 12 wt. % amorphous SiO_2, were synthesized for the neutron scattering experiments according to a sintering procedure described previously by Otto and Meibohm,[14] using dehydrated (black) dioptase $Cu_6Si_6O_{18}$ as a starting material. Unfortunately, a route for the synthesis of the pure polysilicate $CuSiO_3$ does not exist up to now. The multiphase nature of the sample and the small size and anisotropic form of the crystallites of the main phase introduce some difficulties into the evaluation of the diffractograms obtained. The small content of amorphous SiO_2 causes a modulation of the background in addition to the contributions from the cryostat and sample support material. Furthermore, CuO contributes because of its antiferromagnetic phase transition at $T_N = 220$ K (Refs. 23, 24) both broad Bragg reflections and superstructure reflections. In addition, a small relic of the black dioptase starting material, although less than 2 wt. % of the whole sample, could be detected. Some of these reflections almost coincide with magnetic superstructure reflections of the copper polysilicate main phase. A thorough scaling of this phase is needed in order to avoid a wrong fit of displacement coefficients for the main phase atoms. Finally, the main phase reflections may be broadened in two ways; in addition to effects of the small size and elongated crystallite shape there exists an influence on the linewidths due to strain which is partially caused by an intergrowth between $CuSiO_3$ and CuO.[14]

The neutron diffraction experiments were performed on two different two-axis powder diffractometers at the Orphee reactor of Laboratoire Léon Brillouin (LLB), Saclay. Measurements on the thermal beam tube high resolution 3*T*-2 diffractometer were done at room temperature, 15 K ($T > T_N = 8$ K) and 5 K ($T < T_N$) in the scattering angle range from 7° to 114° in 2 Θ, step width 0.05° (2Θ), using an incident wavelength of $\lambda = 1.2251$ Å selected by a Ge(335) monochromator. These diffractograms include 244 main phase reflections. In addition, a larger number of diffraction patterns was recorded in order to characterize the less intense superstructure reflections of $CuSiO_3$ below the second order phase transition. These measurements were done at seven selected temperatures from 14.9 down to 1.4 K on the cold neutron guide *G*4-1 high flux powder diffractometer ($\lambda = 2.4266$ Å, focusing pyrolithic graphite monochromator) in the scattering angle range from 0 up to 125° in 2 Θ and with a step width of 0.1° (2 Θ). The diffractograms cover 22 main phase reflections.

III. RESULTS

The neutron powder data measured were evaluated through the Rietveld technique to obtain the most reliably refined structural and magnetic data using room temperature starting parameters from x-ray results for the $CuSiO_3$ main phase and the minor phase CuO and black dioptase, $Cu_6Si_6O_{18}$, as a relic.[14,23–25] The refinements are performed with the aid of the FULLPROF program package, applying a Thompson-Cox-Hasting pseudo-Voigt profile function.[26] Owing to the lack of experimental low temperature data the minor phases CuO and black dioptase were considered as perturbation and some parameters, structural and magnetic, were fixed in the course of the refinement of the low temperature data sets in order to restrict the number of free parameters. The very short periodicity along the chain axis indicating strong bonding favours a needle habit. So the best profile fits could be performed by choosing a [001] elongated needle shape for the $CuSiO_3$ crystallites with a habitus aspect ratio of about 2.7 in order to correct for different half-peak widths of the reflections. Results for the refined lattice parameters and structural parameters of $CuSiO_3$ are summarized in the Tables I and II. All the atomic sites were found to be fully occupied in the limit of the estimated standard deviations. The derived bond lengths, bond strengths[27] and angles as well as thermal displacement data are given in the Tables III and IV. Experimental patterns for selected temperatures are depicted in the Figs. 1 and 2, showing at the bottom the differences between observed and calculated step intensities. Thermal ellipsoid plots are illustrated with the ORTEP-III (1.0.3) program for WINDOWS[28] in Figs. 3 and 4. The quantitative phase analysis revealed a content of about 80 wt. % of $CuSiO_3$, 18 wt. % of CuO, and less than 2 wt. %

TABLE I. Temperature dependence of the lattice parameters p for $CuSiO_3$ in comparison to $CuGeO_3$.

p	295 K	15 K	5 K	$\Delta p/p$ (%)	Reference
			$CuSiO_3$		
a (Å)	4.6343(4)	4.6224(4)	4.6227(4)	+0.25	
b (Å)	8.7802(7)	8.7464(7)	8.7448(7)	+0.40	this work
c (Å)	2.8330(2)	2.8338(2)	2.8338(2)	−0.03	
V (Å^3)	115.28(2)	114.57(2)	114.56(2)	+0.62	
			$CuGeO_3$		
a (Å)	4.7956(13)	4.7892(8)	4.7894(12)	+0.13	
b (Å)	8.466(4)	8.402(6)	8.402(5)	+0.76	(Ref. 20)
c (Å)	2.9404(13)	2.9444(7)	2.9445(13)	−0.14	
V (Å^3)	119.38(10)	118.48(11)	118.49(10)	+0.74	

of black dioptase, considering only the crystalline phases.

Magnetic scattering gives only a weak contribution to the high resolution pattern but may be easily followed with the high flux diffractometer. We have collected diffraction patterns at 14.9 K ($T > T_N$) and below the Néel point, $T_N = 8$ K, as shown in the Figs. 5 and 6. Two weak reflections of magnetic origin can be clearly identified in the low scattering angle part of the records below T_N. They can be indexed as satellites to the ordinary 110 Bragg reflection of $CuSiO_3$ with a commensurate propagation vector of $\mathbf{q} = (1/2, 0, 1/8)$. We

TABLE II. Result of the structural analyses of $CuSiO_3$ at selected temperatures. Numbers in parentheses are the estimated standard deviations in the units of the least significant digit given. The displacement coefficients U (isotropic) or U_{ij} (anisotropic) are given in Å^2 units. The displacement factor is $T = \exp\{-2\pi^2 \Sigma U_{ij} h_i h_j a_i^* a_j^*\}$, where $U_{13} = U_{23} = 0$. Reliability factors R_{Bragg} as well as profile parameters R_p and R_{wp} are given at the bottom of the table.[26] DW represents the estimated value of the Durbin-Watson statistics.[29]

Parameter		X-ray (Ref. 14)	Neutron		
		295 K	300 K	15 K	5 K
Cu	x	0.5	0.5	0.5	0.5
	y	0	0	0	0
	z	0	0	0	0
	U_{11}	0.059(4)	0.0265(2)	0.0127(13)	0.0133(13)
	U_{22}	0.042(4)	0.0258(11)	0.0130(10)	0.0132(10)
	U_{33}	0.012(3)	0.0014(8)	0.0010(9)	0.0012(9)
	U_{12}	0.027(3)	0.0055(9)	0.0056(8)	0.0055(8)
Si	x	0.0962(2)	0.0975(6)	0.0957(6)	0.0963(6)
	y	0.25	0.25	0.25	0.25
	z	0.5	0.5	0.5	0.5
	U	0.026(3)	0.0095(7)	0.0042(7)	0.0055(7)
O(1)	x	0.918(3)	0.9129(6)	0.9076(6)	0.9079(6)
	y	0.25	0.25	0.25	0.25
	z	0	0	0	0
	U	0.009(5)	0.0071(5)	0.0050(5)	0.0057(5)
O(2)	x	0.285(2)	0.2953(5)	0.2906(4)	0.2909(4)
	y	0.0999(9)	0.0991(3)	0.0980(3)	0.0977(3)
	z	0.5	0.5	0.5	0.5
	U_{11}	0.030(9)	0.0283(13)	0.0127(11)	0.0113(11)
	U_{22}	0.045(10)	0.0209(9)	0.0122(9)	0.0107(8)
	U_{33}	0.006(4)	0.0079(7)	0.0027(8)	0.0042(8)
	U_{12}	0.004(8)	0.0200(9)	0.0089(9)	0.0094(8)
R_{Bragg}	(%)	1.50	2.34	2.42	2.40
R_p	(%)	4.20	7.64	7.23	7.47
R_{wp}	(%)	5.20	8.00	7.57	7.89
DW		0.65	0.93	0.87	0.92

TABLE III. Bond lengths (Å) and angles for $CuSiO_3$ at selected temperatures as well as further interatomic distances and angles important for the comparative interpretation. The nomenclature of the different angles corresponds to that given by Braden *et al.* (Ref. 20). Bond valences *s* are calculated according to Brown and Shannon (Ref. 27). O(1) bridging oxygen atom, O(2) terminal oxygen atom of the silicate chain. Standard deviations given for the 5 K data in parentheses are also valid for the 300 and 15 K data sets.

Atoms	300 K distances (angles)	*s*	15 K distances (angles)	*s*	5 K distances (angles)	*s*
Cu–O(1)×2	2.9120	0.042	2.8864	0.044	2.8871(14)	0.044
Cu–O(2)×4	1.9139	0.523	1.9179	0.517	1.9162(11)	0.519
Σ_s		2.17		2.15		2.16
Si–O(1)×2	1.6548	0.908	1.6623	0.889	1.6632(17)	0.887
Si–O(2)×2	1.6113	1.024	1.6062	1.039	1.6073(22)	1.036
Σ_s		3.87		3.86		3.85
O(1)–O(1)$\parallel c$	2.8330		2.8338		2.8338(4)	
O(2)–O(2)$\parallel c$	2.8330		2.8338		2.8338(4)	
O(2)–O(2)$\parallel b$ (tetr.)	2.6500		2.6594		2.6637(23)	
O(2)–O(2)$\parallel$(001) (oct.)	2.5742		2.5853		2.5799(23)	
O(1)–O(2)	2.6274		2.6286		2.6300(20)	
α O(1)–Cu–$O(2)_{proj}$	88.55		89.23		89.30(9)	
β Cu–O(1)–Cu	97.84		98.50		98.44(4)	
γ O(2)–Si–O(2)	110.64		111.75		111.92(18)	
δ Cu–O(2)–Si_{proj}	167.21		165.64		165.52(13)	
ε Cu–O(1) onto *a*	48.92		49.25		49.22(5)	
φ O(1)–Si–O(1)	117.74		116.94		116.85(9)	
φ' O(1)–Si–O(2)	107.11		107.06		107.05(15)	
τ O(2)–O(2) onto *a*	42.53		41.52		41.48(5)	
η Cu–O(2)–Cu	95.48		95.25		95.37(5)	
$\sigma \langle$|O-Si-O-109.47°|$\rangle$	3.15		3.23		3.25	

notice with respect to the zero q_y component that for the space group *Pbmm* the structural motive is already repeated along the *b* direction by the action of the glide mirror plane perpendicular to the *a* axis with *b*/2 glide component. Figure 7 shows the temperature dependence of the integrated neutron diffraction intensity $I_m(T)$ of the strongest $[1/2,1,-1/8]$ magnetic satellite for $CuSiO_3$ giving clear evidence for the onset of magnetic scattering at about $T_N=8.0$ K. The integrated magnetic reflection intensity scales with the square of the ordered moment $I_m(T)\propto\mu^2$. In view of the fact that the phase transition starts at a very low temperature it is difficult to tell apart the critical behavior and beginning of the saturation of the order parameter. In the asymptotic critical region near T_N the temperature dependence of the intensities may be described by a critical magnetic exponent β_m. In a convincing x-ray diffraction study of critical phenomena at the spin-Peierls transition in isotopic $CuGeO_3$, Lumsden *et al.*[30] indicated a rather narrow asymptotic critical region and obtained the best fit of the intensity data to a modified power law of the reduced temperature $t=1-T/T_{sp}$ according to $I(T)=I_0t^{2\beta}(1+At^{0.5})$, yielding an exponent of $\beta=0.345(30)$ at a transition temperature of $T_{sp}=14.05(1)$ K. This value of β is consistent with 3D *XY* universality.[31–33] Although our intensity data for $CuSiO_3$ have been measured much less densely in the asymptotic region near T_N, we were able to fit the data with a similar result for β_m using the same modified power law with the first correction-to-scaling term included (Fig. 7). The critical exponent obtained is $\beta_m=0.34(3)$ at a Néel temperature of $T_N=8.01(5)$ K. As with other inconsistent values of the critical exponent reported for $CuGeO_3$, our first fit to a simple power law yielded a misleading value of $\beta_m=0.25(4)$ at $T_N=7.8$ K.[34,35]

From the scaling of the magnetic onto the nuclear Bragg intensities, we obtained for the experimental magnetic moment at $T=1.4$ K a value as high as $\mu_z=0.83(2)\mu_B$, when attributing the magnetic moment to the hole on the $3d^9$ copper site with spin alignment along the *z* direction. A slightly larger value of $\mu_x=1.09(3)\mu_B$ with a deceptively good fit reliability ($R_{mag}=3.6\%$) was determined for spin alignment along the *x* direction. With the little scattering information, a definite determination of the ordered moment and especially its orientation is difficult. At first sight one may discard the orientation along *x* due to its physically questionable high ordered moment. On the other hand, on the basis of a reliably observed intensity of the magnetic single peak with $d=2.343$ Å it would be possible to decide whether the spin alignment is along the *x* or the *z* direction, because the calculated intensities for the two possibilities of spin orientation result in a ratio of about 10:1 (Table V). Figure 8 shows the neutron scattering difference intensity obtained by subtraction of measurements with magnetic scattering from those

TABLE IV. Size and orientation of the atomic displacement ellipsoids for $CuSiO_3$

T (K)	Atom	Principal displacements (r.m.s. amplitudes in Å)	Angles (deg.) between ellipsoid and unit-cell axes		
			a	b	c
300	Cu	0.178	43.1	46.9	90
		0.144	46.9	−43.1	90
		0.038	90	90	0
	Si	0.092	90	0	90
		0.127	0	90	90
		0.062	90	90	0
	O(1)	0.111	90	0	90
		0.056	0	90	90
		0.077	90	90	0
	O(2)	0.212	39.8	50.2	90
		0.065	50.2	−39.8	90
		0.089	90	90	0
15	Cu	0.135	45.7	44.3	90
		0.076	44.3	−45.7	90
		0.032	90	90	0
	Si	0.077	90	0	90
		0.070	0	90	90
		0.038	90	90	0
	O(1)	0.066	90	0	90
		0.080	0	90	90
		0.063	90	90	0
	O(2)	0.144	44.1	45.9	90
		0.057	45.9	−44.2	90
		0.063	90	90	0
5	Cu	0.137	44.6	45.4	90
		0.083	45.4	−44.6	90
		0.034	90	90	0
	Si	0.095	90	0	90
		0.057	0	90	90
		0.038	90	90	0
	O(1)	0.091	90	0	90
		0.073	0	90	90
		0.057	90	90	0
	O(2)	0.143	44.1	45.9	90
		0.039	45.9	−44.1	90
		0.065	90	90	0

without a magnetic scattering contribution after suitable scaling. Exploiting the remarkable width of genuine magnetic peaks with full width at half maximum FWHM(2Θ)≈0.5° in comparison with the 0.1° step width, we were able to discriminate between such peaks and the background noise by convolving the difference diagram with a smoothing function. In this way, at least four magnetic peaks could be significantly measured, the intensity of which exceeds its fivefold uncertainty. The diagram clearly indicates magnetic scattering intensity of the examined peak with $d=2.343$ Å in an amount that favours x spin alignment and does not show evidence of z spin direction, although the decisive estimation may be slightly influenced by artefacts of intense Bragg peaks.

IV. DISCUSSION

The single chain silicate $CuSiO_3$ is the unique example of anhydrous silicates of copper, apart from completely dehydrated dioptase (black dioptase) with the same chemical composition. The competing network forming cations Cu^{2+} and Si^{4+} both share chains down [001] in this orthorhombic crystal structure as a result of almost identical length of the tetrahedral edge for SiO_4 and the distance between edges of the ''octahedral'' basis of the CuO_{4+2} polyhedron (Fig. 9). On the other hand, even the misfit between the two chain periods may lead to a strained crystal structure.

The dependence of structural parameters on temperature in $CuSiO_3$ (Tables I–III) is remarkably similar to that ob-

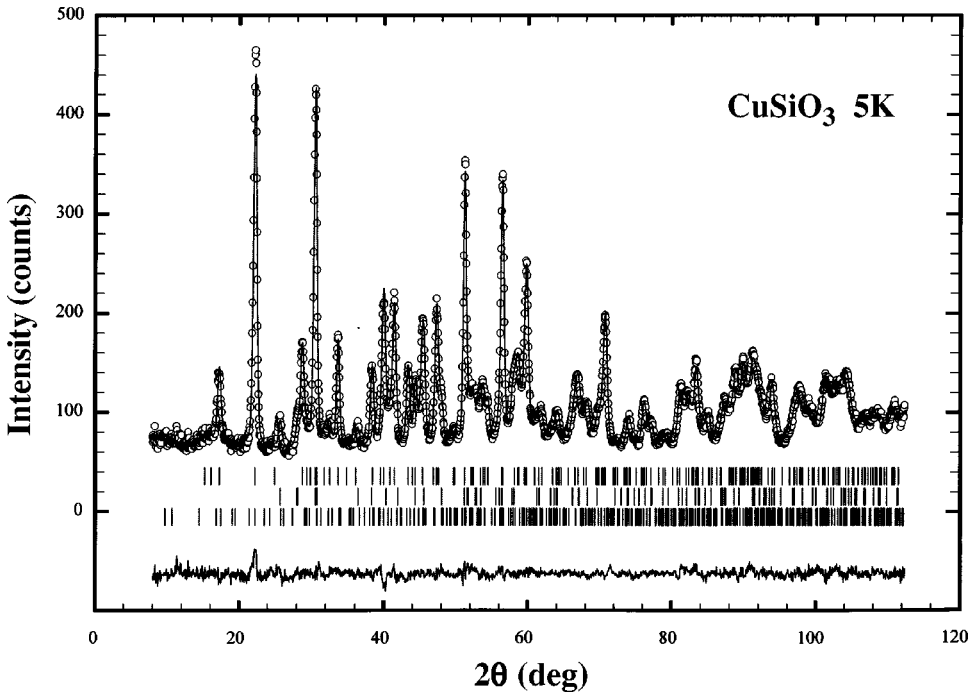

FIG. 1. High resolution neutron diffraction record of the multiphase sample with the main compound $CuSiO_3$ at 5 K ($\lambda = 1.2151$ Å). The bar diagrams below indicate peak positions of the main phase, CuO and black dioptase. The difference between observed and calculated step intensities is depicted at the bottom.

served in $CuGeO_3$.[20,21] Both compounds should be considered as nearly planar quasi-two-dimensional crystal structures with the layers being deformed into a zig-zag arrangement (Figs. 10 and 11). The thermal expansion of a layered structure is expected to be manifested mainly in the distance between the layers, in addition the zig-zag folding of the layers allows for efficient contraction by an enhancement of the zig-zag angle upon cooling. This describes very well the main part of the temperature induced structural changes. In both compounds, one finds a very similar temperature related rotation of the CuO_2 ribbons around the *c* axis. The angle τ (Fig. 10) decreases by about 1° in the silicate and by about 0.7° in the germanate and consequently the folding angle $\beta = 2\varepsilon$ increases upon cooling in both materials. Whereas these rather large effects are well understood with purely structural arguments for both compounds, the germanate exhibits at low-temperature additional thermal expansion anomalies.[22] These are characterized by a remarkable increase in the *c* parameter and a merely moderate decrease in the *a* lattice parameter in comparison with the silicate. These effects arise from the strong magnetoelastic coupling in $CuGeO_3$: at lower temperatures magnetic coupling becomes important and an enhancement of the magnetic exchange parameter yields a decrease in free energy.

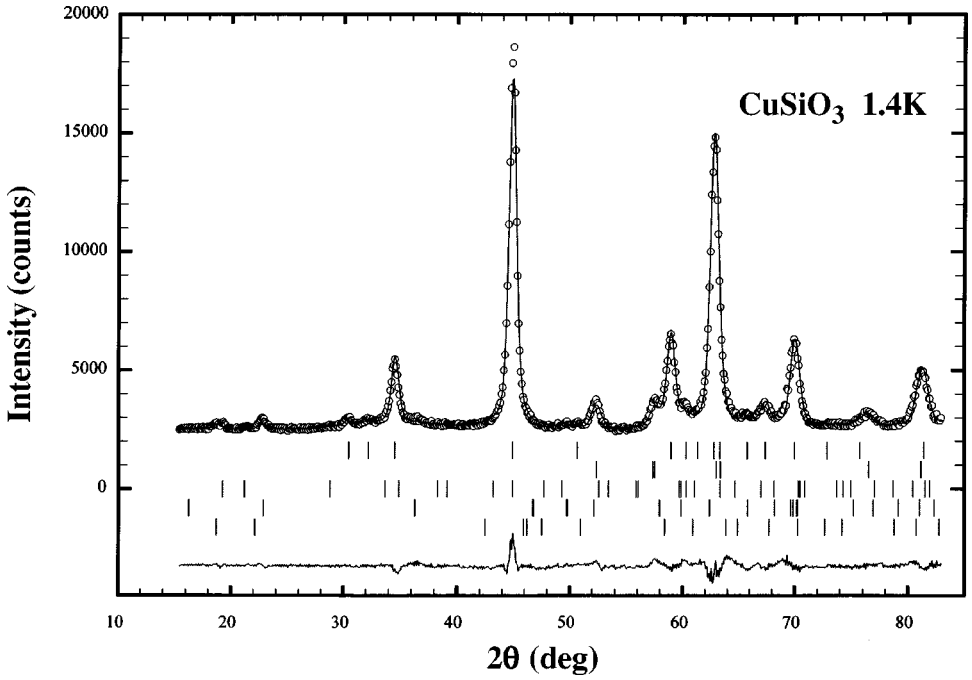

FIG. 2. High flux neutron diffraction record of the multiphase sample with the main phase $CuSiO_3$ at 1.4 K ($\lambda = 2.4266$ Å). Three structural and two magnetic intensity contributions were taken into account in the data fit. Their peak positions are indicated in the bar diagrams below reading from top to bottom: $CuSiO_3$, CuO, $Cu_6Si_6O_{18}$ relic, and then magnetic parts of $CuSiO_3$ and CuO.

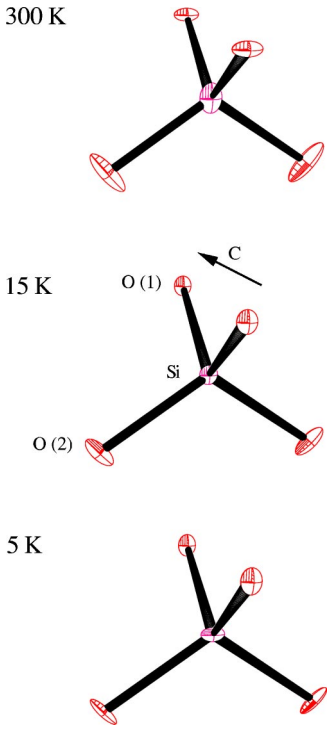

FIG. 3. Thermal ellipsoids (ORTEP plot) of the coordination tetrahedron around Si for different temperatures.

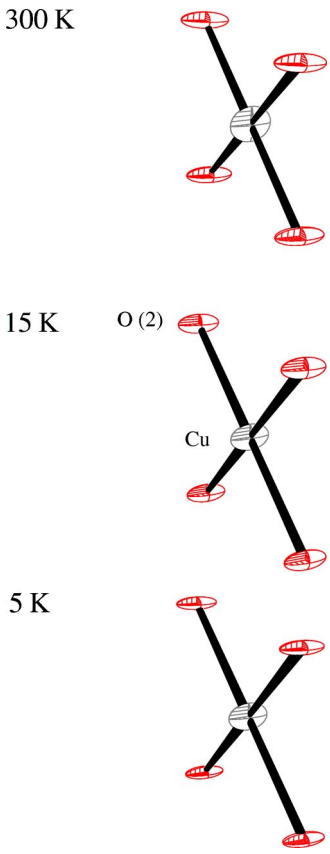

FIG. 4. Thermal ellipsoids (ORTEP plot) of the Cu-O(2) plaquette for different temperatures.

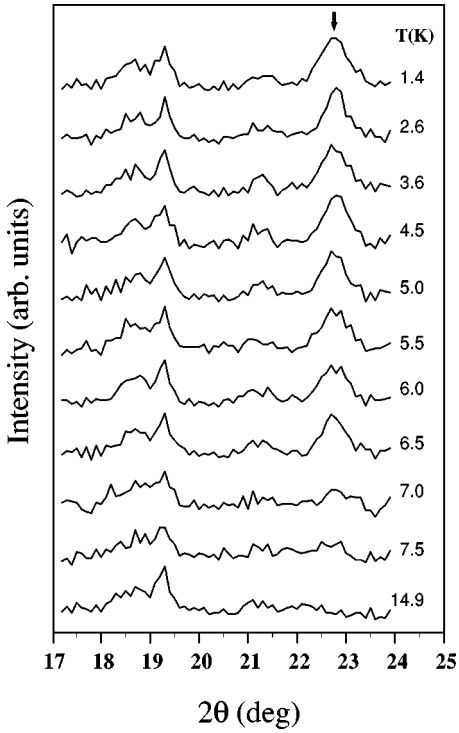

FIG. 5. Low scattering angle detail of the 11 temperature scan diffractograms recorded with the high flux G4-1 diffractometer ($\lambda = 2.4266$ Å). Near $2\theta = 22.9°$ the strongest magnetic peak appears, when the temperature crosses $T_N = 8$ K.

The enhancement of the magnetic exchange parameter may be achieved with minor deformations of the CuO_2 arrangement associated with the anomalies in the thermal expansion.

A glance at Table I shows the temperature dependence of the orthorhombic lattice parameters obtained from neutron diffraction data for $CuSiO_3$ together with results for $CuGeO_3$ for comparison.[20] Whereas the periodicities along the *a* and *b* directions decrease with decreasing temperature, the periodicity down the chain direction *c* increases only slightly in contrast to $CuGeO_3$. The chain arrangement in $CuSiO_3$ with its very short translation period is extremely stiff and obviously does not allow any large alteration with temperature. As for $CuGeO_3$ the pronounced change in the *b* axis parameter may also be evidence of a ''soft'' *b* direction for $CuSiO_3$. According to results from the high flux data obtained at different temperatures below 15 K, a significant change in the lattice parameters could not be proved, when the temperature crosses the phase transition at $T_N = 8$ K. The anomalous effects observed in the germanate are obviously absent in the silicate. This strongly suggests that the silicate is not a magnetically one-dimensional system with a comparable exchange interaction in agreement with the conclusion obtained from the antiferromagnetic propagation vector.

Turning to crystal-chemical results, the trend of the bond valence sums towards values calculated too high for Cu^{2+} and too low for Ge^{4+} is more pronounced for $CuSiO_3$ (Table III) than for $CuGeO_3$.[20] Giving the mean for the neutron scattering data sets measured at different temperatures, we find 2.16 instead of the 2+ valence for Cu and 3.86 instead of the 4+ valence for Si; the values reported for $CuGeO_3$ are

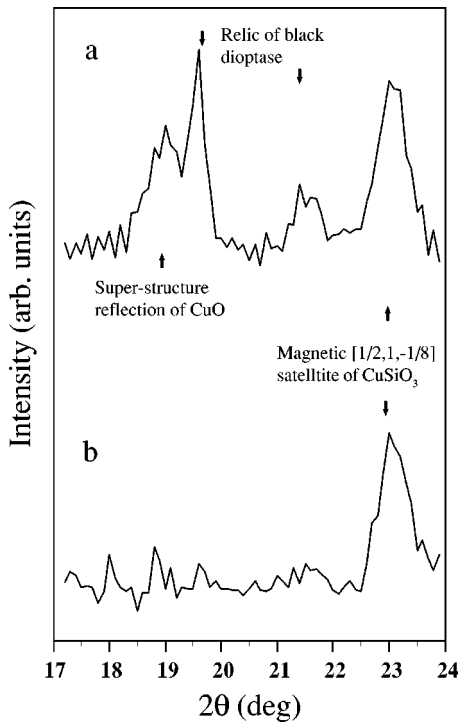

FIG. 6. Sum and difference curves using neutron diffraction data in order to clearly illustrate and characterize the weak superstructure and secondary phase reflections in the low scattering angle range: (a) sum curve of 11 temperature scan diagrams recorded from $T=1.4$ K to 14.9 K; (b) difference curve of the eight lower temperature records (1.4 to 6.5 K) minus the three higher temperature diagrams (7 to 14.9 K) after adequate scaling, showing solely the foremost [1/2, 1, −1/8] super-structure reflection of magnetic origin below $T_N=8$ K.

2.13 and 3.94, respectively. If we deal with very anisotropic displacements of atoms, and this is the case especially for $CuSiO_3$, the bond lengths are actually enlarged and in turn the bond valence sum is indeed smaller than derived from the central distances only. In addition, the crystal structure of $CuSiO_3$ is strained both sterically with respect to the Si surrounding and electronically with respect to the anisotropy related to the huge Jahn-Teller distortion around Cu^{2+}. This can explain the discrepancies in the bond valences found. On the other hand, it is the x-ray diffraction method, from which in general the coefficients for bond-valence–bond-length relations are derived. Because neutrons probe the atomic core whereas x rays measure the center of gravity of the electron shell, there may exist especially for strongly polarizable ions such as oxygen a difference in the derived atomic locations comparing results of both methods. This can explain at least partially misleading bond valence sums in the case of neutron diffraction. The discrepancy between x-ray and neutron results for $CuSiO_3$ may be understood in this sense, pointing to the possibility of gradually polarized O(2) oxygen atoms in view of their acentric positions of site symmetry *m*.

From the structural data obtained one can prove that in the silicate single chain, representing the most stretched case of all silicate chains,[36] the covalent bonding character between silicon and oxygen is highly enhanced at the expense of the ionic part. The Si-O_{br}-Si valence angle of $\varphi=117.7°$ at room temperature (116.9° at 5 K) represents the ultimate limit observed for condensed silicate anions, compared to the most frequent 139° angle determined from a large number of accurate silicate data sets.[37,38] The six O-Si-O valence angles, having values of $4\times107.1(1)°$, 110.6(1)°, and at least 117.7(1)°, deviate in the mean only about $\sigma=3.2°$ from the ideal 109.47° tetrahedral angle indicative for strongest sp^3 hybridization of Si^{4+} (Table III) and in turn for a rather strong *sp* hybridization of oxygen. This information is important in view of recent ^{29}Si NMR measurements indicating that the Si-O(2) path is strongly involved in the magnetic exchange interaction below T_N.[39] The corresponding O(2)-Si-O(2) valence angle γ is considerably increased with temperature decrease; its change from 15 down to 5 K was about 0.2° (Table III).

In accordance with crystal-chemical rules and common experiences, the copper coordination, representing a very strongly elongated Jahn-Teller ''octahedron,'' is typical for copper in the $3d^9$ state with the unpaired electron in the $3d_{x^2-y^2}$ orbital. The four short Cu-O(2) bond distances increase, but not significantly, from 1.9139(11) to 1.9162(11) Å, when the temperature is reduced from room temperature down to 5 K, whereas the alteration of the two long Cu-O(1) bond distances goes in the opposite direction from 2.9120(14) to 2.8871(14) Å. Near the transition temperature

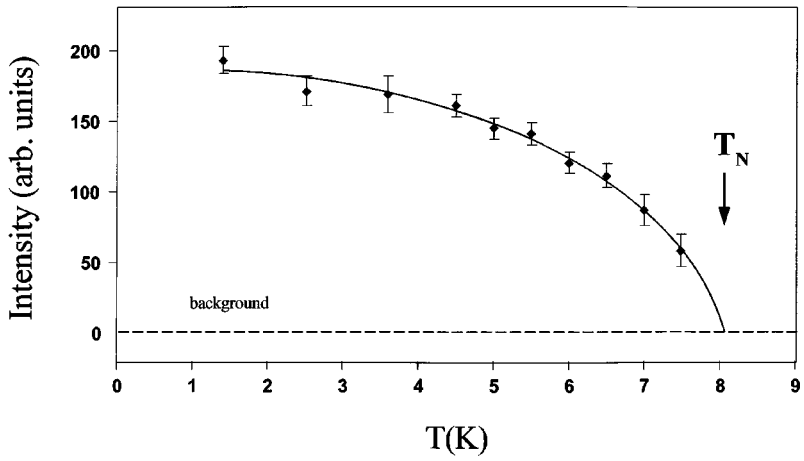

FIG. 7. Temperature dependence of the integrated magnetic neutron diffraction intensities I_m for the [1/2, 1, −1/8] satellite ($d=6.121$ Å) of $CuSiO_3$. The solid line represents the fit of I_m to a power law in the reduced temperature $t=1-T/T_N$ modified by the first correction-to-scaling term according to $I_m=I_0t^{2\beta}(1+At^{0.5})$: $\beta=0.34(3)$, $A=-0.55(3)$, $I_{T=0}=I_0(1+A)=196$.

TABLE V. Comparison of the observed and calculated intensities of magnetic reflections derived from high flux diffractometer data at 1.4 K for $CuSiO_3$. The reflections are indexed using the scattering vector $\mathbf{h}=\mathbf{H}+\mathbf{q}$, where $\mathbf{H}$ is the reciprocal lattice vector of the chemical unit cell and $\mathbf{q}=(1/2,0,1/8)$ is the propagation vector. k is always an odd integer due to the motive doubling in the b direction for the *Pbmm* space group. The magnetic moment with spin alignment along the x direction resulted in $\mu_x=1.09(3)\mu_B$ ($R_{\mathrm{mag}}=3.6\%$), spin alignment down the z direction yielded a magnetic moment of $\mu_z=0.83(2)\mu_B$ ($R_{\mathrm{mag}}=6.4\%$). The fits using the difference diagram depicted in Fig. 8 gave less reliable results with $R_{\mathrm{mag}}=12\%$ for the x spin direction and $R_{\mathrm{mag}}=30\%$ for the z spin direction.

I_{obs}	$I_{\mathrm{calc}}(x)$	$I_{\mathrm{calc}}(z)$	d (Å)	H	K	L	h	k	l
109	109	109	6.1180	1	1	0	1/2	1	−1/8
39	35	5	2.8865	1	1	1	1/2	1	7/8
	4	20	2.8830	1	1	0	3/2	1	1/8
27	29	18	2.7596	1	3	0	1/2	3	−1/8
21	20	2	2.3426	−1	1	1	−1/2	1	9/8
8	10	5	2.1636	−1	1	1	−3/2	1	7/8
21	14	5	2.1100	1	3	1	1/2	3	7/8
	7	8	2.1087	1	3	0	3/2	3	1/8
7	6	3	1.9041	1	1	1	3/2	1	9/8
10	10	3	1.8672	−1	3	1	−1/2	3	9/8

T_N a flat maximum (minimum) in the bond distances is observed (Table III).

Turning to the surrounding of the oxygen atoms, the O(1) atom is found in a distorted tetrahedral environment of two Si and two Cu atoms, in this way forming sp^3 hybridized orbitals. More interesting of course in view of the magnetic properties is the nearly planar arrangement of cations around the oxygen O(2) with one Si and two Cu atoms forming valence angles Cu-O(2)-Cu of 95.4° and Cu-O(2)-Si of $2\times130.7°$.

In general, the mean-square displacements for all atoms are similar for both $CuGeO_3$ (Ref. 20) and $CuSiO_3$ (Table IV) showing the smallest component down the chain direction with its very short periodicity and, only for Cu and O(2), strongly anisotropic displacements orthogonal to this direction. The largest principal axis of the displacement ellipsoids for the oxygen atoms belonging to the Si coordination sphere lies almost perpendicular to the directions of covalent bonding and are again indicative of very strong bonds (Fig. 3). The Cu and O(2) atoms forming the coordination ''octahedron'' basis show their largest displacement almost in the direction normal to this basis, deviating only a few degrees from the angle $\varepsilon\approx49°$, which represents the angle between the Cu-O(1) direction and the a axis. In this way the O(2) atoms obviously move in the ab plane towards two empty structural channels, which are formed down [001], the first intersecting the unit-cell origin and the second the coordinates $x=1/2$, $y=1/4$ on the mirror plane (Fig. 9).

The reduction of the displacement amplitudes with temperature happens to be quite normal at first sight (Figs. 3 and 4). But the still remarkable residual atomic displacements for O(2) and Cu perpendicular to the plaquettes at low tempera-

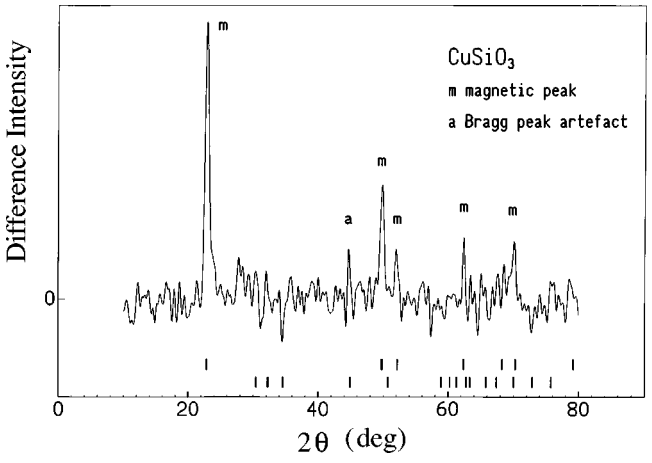

FIG. 8. Representation of magnetic peaks using a difference diagram and the scaling procedure according to that of Fig. 6 (curve b). Bar diagrams at the bottom indicate the position of magnetic peaks and of possible Bragg peak artifacts.

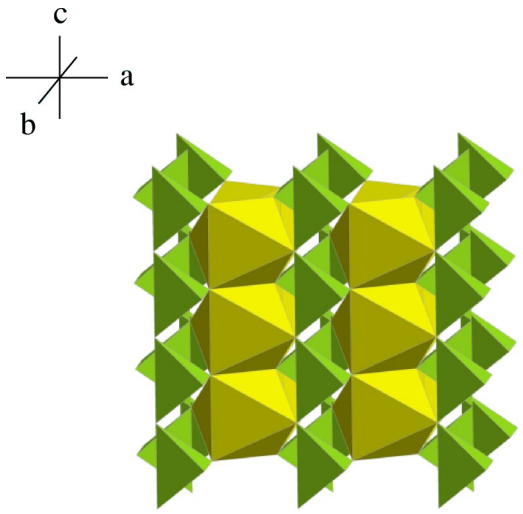

FIG. 9. Picture of the crystal structure of $CuSiO_3$ showing the connection of silicate and cuprate chains running down the c axis.

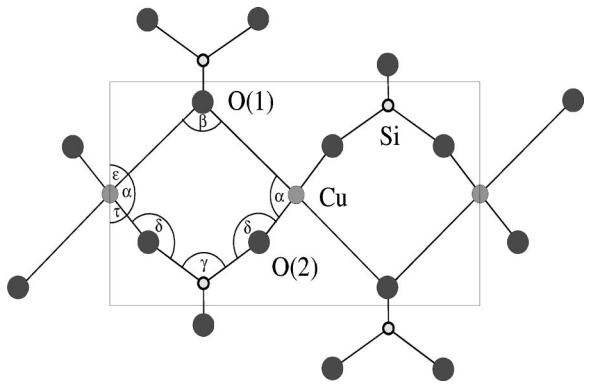

FIG. 10. Projection of the crystal structure of $CuSiO_3$ along *c* showing the different angles in discussion (Refs. 20, 21).

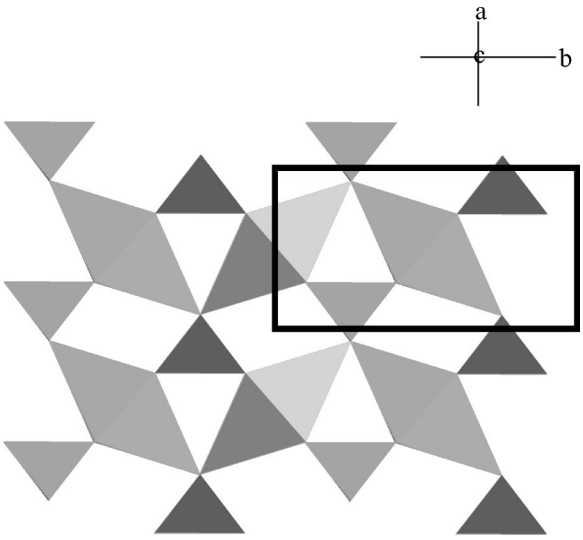

FIG. 11. Polyhedra drawing of the crystal structure of $CuSiO_3$ as projection down [001] showing the empty structural channels. The projected unit cell is outlined.

ture may suggest that a predisposition for a structural transformation as found for $CuGeO_3$ is intrinsically imposed in the $CuSiO_3$ system too. In case of a completely statistical ordering of the atomic split positions, which characterize the spin-Peierls transition in $CuGeO_3$, a similar feature for both amplitude and direction of atomic principal displacement as found for $CuSiO_3$ would result for the prototypic structure. The reason why such a magnetically induced phonon mode does not condense at low temperature in $CuSiO_3$ may be indeed the markedly reduced *c* periodicity as a consequence of ''chemical pressure'' caused by the substitution of the Ge^{4+} by the smaller Si^{4+}. Even though the *ab* plane O(2)-O(2) distance in $CuSiO_3$ is already considerably increased in comparison to $CuGeO_3$, there is no real possibility for the copper atom to move in the [001] direction as copper does by the magnetoelastic spin-Peierls transition in $CuGeO_3$.

The oxygen atoms around Cu in the form of a flattened tetrahedron may be modeled from the strongly vibrating O(2) atoms, which would suggest some charge transfer towards monovalent copper. But a vibrational mode transforming the O(2) plaquette into such a tetrahedron is forbidden due to the mirror symmetry perpendicular to *c* in the *Pbmm* space group.

Considering the magnetic properties, the main antiferromagnetic interaction is attributed to the Cu-O(2)-Cu superexchange path. According to the Goodenough-Kanamori-Anderson rule this interaction is stronger the more the Cu-O(2)-Cu bond angle η deviates from the 90° case.[40] In the near 90° configuration, in which the O(2)-O(2) separations of the $CuO(2)_2$ plaquette along the *c* direction (L_c) and in the *ab* plane (L_{ab}) would be almost equal, a small or negligible antiferromagnetic interaction would enter in competition with a ferromagnetic contribution. We obtain for $CuGeO_3$ an aspect ratio $L_c/L_{ab}=2.9446/2.5072=1.174$, using the mean values of the O(2) split positions at 4 K,[20] and for $CuSiO_3$ at 5 K $L_c/L_{ab}=2.8338/2.5799=1.098$. The corresponding bond angles, most relevant for the magnetism, are clearly different to 90° giving $\eta=99.2°$ for $CuGeO_3$ and just $\eta=95.4°$ for $CuSiO_3$.

The observation of an antiferromagnetic ordering with propagation vector (1/2, 0, 1/8) contradicts the first interpretation of $CuSiO_3$ deduced from macroscopic measurements which suggested a dominant but weak antiferromagnetic interaction along the chain direction.[16] We have tested several magnetic ordering schemes with antiferromagnetic coupling along the chain, but they do not explain the magnetic reflections observed at low *Q* value. From the long modulation along the chain one has to deduce that nearest-neighbor magnetic exchange is ferromagnetic in nature. This is not that astonishing in view of the slightly different CuO_2 arrangement and the extremely high sensitivity of the magnetic exchange to minor structural deformations. In $CuGeO_3$ the Cu-O(2)-Cu angle of 99° yielded an antiferromagnetic exchange parameter of $J=13$ meV, and the dependence of J_{nn} on this angle was calculated in detail in order to explain the dimerization in the spin-Peierls phase.[20] Taking these results one would expect a ferromagnetic exchange interaction in $CuSiO_3$ with the Cu-O(2)-Cu angle of only 95°. However, the next-nearest-neighbor coupling J_{nnn} should not be very much different in the two compounds. Therefore, one would expect a still antiferromagnetic J_{nnn} in $CuSiO_3$, and also higher interactions should remain antiferromagnetic. Thereby, one may understand the long period of $8\times c$ observed for the magnetic ordering in $CuSiO_3$. Structurally similar CuO_2 chains are also found in the spin ladder compounds, in particular in $La_{14-x}Ca_xCu_{24}O_{41}$. This material also exhibits an antiferromagnetic ordering at low temperature ($T_N=10.5$ K) with a ferromagnetic coupling along the chains.[41] Furthermore, the temperature dependence of the magnetic susceptibility in this compound closely resembles that of $CuSiO_3$ giving further support to our interpretation. The size of the ordered moment in $CuSiO_3$ appears somewhat high compared to the expected reduction of the moment due to quantum fluctuations. In the refined model, we assume a sinusoidal modulation of the spin density, which actually might not be justified in $CuSiO_3$. If the long range period results from a periodic switching of ferromagnetic fragments

across domain boundaries, the refined ordered moment is overestimated with the sinusoidal model. Therefore, the high value of the ordered moment should be interpreted as evidence for such nonsinusoidal spin density modulation.

In view of the high polarizability of O^{2-} and the influence of covalency there may exist the possibility that the spin density observed does not reside entirely on Cu^{2+} but partially on O(2) sites, e.g., that charge is transferred from oxygen to copper creating some holes on the O(2) sites and leaving singlet Cu^{1+} with a filled $3d$ shell. Several important features including some experimental evidence of such states were collected recently showing at the moment a still qualitative picture.[39] If we follow the proposed oxygen tunnel dimers and pile up the spins midway between the two O(2) nuclei, we obtain a spin lattice that is shifted half a *c* period with respect to the Cu sublattice. In this case the fit of the ordered magnetic moment would get the same result, apart from the changed magnetic form factors for such an oxygen. Alluding to the possibility of Cu^{1+} formation we stress that every synthesis undertaken to prepare any silicate of Cu^{1+}, reportedly failed.

An other idea may be considered further, regarding the chemical substitutions, which characterize isotypic theoparacelsite. In this compound $As^{5+}_{2/3}H^{1+}_{2/3}$ completely replaces Ge^{4+} (or Si^{4+}) in the prototypic compound, forming OH^- groups with the protons confined in the otherwise empty structural channels.[17] We may ask, whether a similar substitution of protons at least in a fairly small amount is possible in copper polysilicate, in this way producing $Cu^{1+}SiO_2(OH)$ 'impurities.' The result would be a highly correlated population of Cu^{1+} and Cu^{2+} ions. The appearance of copper ions with different valences (or mixed-valent states) could explain the dark brownish color of the sample, and it also could be the reason for the long magnetic modulation observed down the *c* direction in $CuSiO_3$. Residual nuclear density is smeared out on the $z=0$ level of the rhombic shaped empty channel down [001]. But we could not decide, whether this is an artifact or stems from, for instance, protons of not more than 1/8 site occupation. In the course of the x-ray analysis reported previously,[14] such small proton amounts would surely have gone undetected as a result of the poor scattering power. Resonance spectroscopic investigations would provide useful further information in order to verify this proposal.

The long-periodic magnetic modulation covering eight periods along *c* of the chemical unit cell may pose the question, whether the crystal structure of $CuSiO_3$ is additionally subjected to a long-range magnetoelastic distortion, for instance, with a halving of the magnetic *c* period. The proposed type of modulation could not be verified experimentally. In this context the work of Hidaka *et al.*[42] is interesting. From the authors the appearance of super-structure reflections at room temperature has been reported for $CuGeO_3$ single crystals, which could be indexed using lattice parameters $2\times a, b, 4\times c$ with respect to the nominal *Pbmm* unit cell. The crystals were annealed at 1423 K in an oxygen atmosphere in order to develop the superstructure. Under an ambient atmosphere, not even under oxygen, the applied high annealing temperature may be sufficient to produce already some Cu^{1+} in addition to Cu^{2+}. A comparative study using a differently synthesized sample could not confirm this $CuGeO_3$ modulation, neither of long-range nor of short-range type.[21]

Finally, the quite small size of the crystallites in the powder sample used may surely affect the magnetic ordering too. From the peak widths of an x-ray diffraction experiment of high resolution, a mean crystallite size in the chain direction could be estimated to be about 500 Å; in the other two directions the size is in fact about two times smaller. Strain effects have been taken into account. For such a semi-infinite $S=1/2$ spin chain it has been proposed that staggered moments near the chain ends would be induced, which may lead to an antiferromagnetic order.[43,44] The narrow crystallite boundaries in *a* and *b* direction may act in a similar way.

In conclusion, it is shown by a neutron scattering study on a powder sample that orthorhombic $CuSiO_3$ is a quasi-one-dimensional compound, which undergoes below $T_N=8$ K a second order phase transition to a long-range antiferromagnetic Néel state order. The magnetic structure can be described by a propagation vector $\mathbf{q}=(1/2, 0, 1/8)$ with respect to the nominal *Pbmm* crystal structure. The in-chain coupling is expected to be ferromagnetic in nature in view of the Cu-O(2)-Cu valence angle of only 95.4° and the long-periodic magnetic modulation along *c*, but the next nearest neighbor exchange coupling may be still antiferromagnetic. The low temperature magnetic moment determined experimentally on condition that the spin density resides fully on the $Cu3d^9$ sites yielded too high a value in comparison with the expected moment suggesting a nonsinusoidal spin density modulation. The question of spin density residing partially or solely on O(2) non-bonding orbitals[39] is beyond the bounds of this first and basically structural study. $CuSiO_3$ with its more densely packed succession of zig-zag sheets down the *a* direction is believed to be closer to an anisotropic 3D structure than the $CuGeO_3$ prototype. This statement is further supported by the small low temperature reduction of the ordered magnetic moment. The extent and the direction of residual principal displacements of atoms at low temperature may give the picture of a short-range, statistically frozen in phonon mode or strain wave in the heavily deformed crystal structure of $CuSiO_3$.

V. OUTLOOK

The assumption of a possible intergrowth between $CuSiO_3$ and CuO built up some hope for improving the sample quality of $CuSiO_3$ by hydrothermal treatment following the thermal decomposition of dioptase, even though this experiment turns out to be time consuming. Indeed, the minor phases in the mixture, CuO (tenorite) and SiO_2 (amorphous), were observed to transform under conditions of about 438 K and 16.5 MPa partly into $CuSiO_3$. The reduction of the half-peak widths of the $CuSiO_3$ reflections and the observed decrease of peak intensities of CuO compared to those of $CuSiO_3$ give evidence that crystallites of $CuSiO_3$ grew broader at the expense of CuO and SiO_2 and are less strained. This experiment shed light on the question about

the thermodynamic stability of $CuSiO_3$, which represents a borderline case in the field of existing anhydrous silicates of metallic elements.[45] With an improved sample quality we would be able to complete especially spectroscopic investigations down to low temperature, which suffer at the moment from not sufficient crystal dimensions. Fundamental questions that have remained unanswered as yet may be solved then.

ACKNOWLEDGMENTS

We acknowledge financial support of the European Community by the Access to Research Infrastructure action of the Improving Human Potential Program. Furthermore, H. H. Otto and H. Wolfram are grateful for the hospitality of the LLB staff at Saclay, France. Work at Cologne University was supported by the DFG through Grant No. SFB 608.

[1] Y. Ginetti, Bull. Soc. Chim. Belg. **63**, 209 (1954).
[2] H. Völlenkle, A. Wittmann, and H. Nowotny, Monatsch. Chem. **98**, 1352 (1967).
[3] M. Hase, I. Terasaki, and K. Uchinokura, Phys. Rev. Lett. **70**, 3651 (1993).
[4] J. P. Boucher and L. P. Regnault, J. Phys. I **6**, 1939 (1996).
[5] S. B. Oseroff, S. W. Cheong, B. Actasi, M. F. Hundly, Z. Fisk, and L. W. Rupp, Jr., Phys. Rev. Lett. **74**, 1450 (1993).
[6] M. Poirier, R. Beaudry, M. Castonguay, M. L. Plumer, G. Quirion, F. S. Razavi, A. Revcolevschi, and G. Dhalenne, Phys. Rev. B **52**, 6971 (1995).
[7] J. P. Renard, K. L. Dang, P. Veillet, G. Dhalenne, A. Revcolevschi, and L. P. Regnault, Europhys. Lett. **30**, 475 (1995).
[8] L. P. Regnault, J. P. Renard, G. Dhalenne, and A. Revcolevschi, Europhys. Lett. **32**, 579 (1995).
[9] M. Weiden, R. Hauptmann, W. Richter, C. Geibel, P. Hellmann, M. Köppen, F. Steglich, M. Fischer, P. Lemmens, G. Güntherodt, A. Grimmel, and G. Nieva, Phys. Rev. B **55**, 15067 (1997).
[10] K.-H. Breuer, Ph.D. thesis, Universität Heidelberg, 1984.
[11] K. Uchinokura, J. Phys. C **14**, R195 (2002).
[12] V. Kiryukhin, B. Keimer, J. P. Hill, and A. Vigliante, Phys. Rev. Lett. **76**, 4608 (1996).
[13] F. Liebau, Z. Phys. Chem. (Leipzig) **206**, 73 (1956).
[14] H. H. Otto and M. Meibohm, Z. Kristallogr. **214**, 558 (1999).
[15] C. Gros, P. Lemmens, K.-Y. Choi, G. Güntherodt, M. Baenitz, and H. H. Otto, Europhys. Lett. **60**, 276 (2002).
[16] M. Baenitz, C. Geibel, M. Dischner, G. Sparn, F. Steglich, H. H. Otto, M. Meibohm, and A. Gipius, Phys. Rev. B **62**, 12201 (2000).
[17] H. H. Otto and H. Wolfram, Z. Kristallogr. **217**, 431 (2002).
[18] J. Sichelschmidt, M. Baenitz, C. Geibel, F. Steglich, A. Loidl, and H. H. Otto, Appl. Magn. Reson. **23**, 75 (2002).
[19] M. Meibohm, H. H. Otto, and W. Brockner, Spectrochim. Acta A (to be published).
[20] M. Braden, G. Wilkendorf, J. Lorenzana, M. Ain, G. J. McIntyre, M. Behruzi, G. Heger, G. Dhalenne, and A. Revcolevschi, Phys. Rev. B **54**, 1105 (1996).
[21] M. Braden, E. Ressouche, B. Büchner, R. Kessler, G. Heger, G. Dhalenne, and A. Revcolevschi, Phys. Rev. B **57**, 11 497 (1998).
[22] H. Winkelmann, E. Gamper, B. Büchner, M. Braden, A. Revcolevschi, and G. Dhalenne, Phys. Rev. B **51**, 12 884 (1995).
[23] S. Åsbrink and L.-N. Norrby, Acta Crystallogr., Sect. B: Struct. Crystallogr. Cryst. Chem. **26**, 8 (1970).
[24] B. N. Brockhouse, Phys. Rev. **94**, 781 (1954).
[25] G. Caglioti, F. P. Ricci, A. Santoro, and V. Scatturin, J. Phys. Soc. Jpn. **17**, Suppl. B-II (1962).
[26] J. Rodrigues-Carvajal, FULLPROF program package, LLB, CEA-CNRS, Saclay, 2000.
[27] I. D. Brown and R. D. Shannon, Acta Crystallogr., Sect. A: Cryst. Phys., Diffr., Theor. Gen. Crystallogr. **29**, 266 (1973).
[28] L. J. Farrugia, J. Appl. Crystallogr. **30**, 565 (1997).
[29] R. J. Hill and H. D. Flack, J. Appl. Crystallogr. **20**, 356 (1987).
[30] M. D. Lumsden, B. D. Gaulin, and H. Dabkowska, Phys. Rev. B **57**, 14 097 (1998).
[31] M. L. Plumer, Phys. Rev. B **53**, 594 (1996).
[32] J. C. le Guillon and J. Zinn-Justin, Phys. Rev. B **21**, 3976 (1980).
[33] K. Hirota, G. Shirane, Q. J. Harris, Q. Feng, R. J. Birgeneau, M. Hase, and K. Uchinokura, Phys. Rev. B **52**, 15 412 (1995).
[34] Q. J. Harris, Q. Feng, R. J. Birgeneau, K. Hirota, K. Kakurai, J. E. Lorenzo, G. Shirane, M. Hase, K. Uchinokura, H. Kojima, I. Tanaka, and Y. Shibuya, Phys. Rev. B **50**, 12 606 (1994).
[35] M. Hase, K. Uchinokura, R. J. Birgeneau, K. Hirota, and G. Shirane, J. Phys. Soc. Jpn. **65**, 1392 (1996).
[36] H. H. Otto, Der Aufşchluß **51**, 47 (2000).
[37] J. A. Tossell and G. V. Gibbs, Acta Crystallogr., Sect. A: Cryst. Phys., Diffr., Theor. Gen. Crystallogr. **34**, 463 (1978).
[38] I. D. Brown, *Structure and Bonding in Crystals*, Vol. II, edited by M. O. Keeffe and A. Navrotsky (Academic Press, New York, 1981).
[39] A. A. Gipius, A. S. Moskvin, M. Baenitz, S.-L. Drechsler, E. N. Morozova, and H. H. Otto, Europhys. Lett. **63**, 282 (2003).
[40] J. B. Goodenough, *Magnetism and Chemical Bond* (Interscience, New York, 1963); P. W. Anderson, Phys. Rev. **115**, 2 (1959).
[41] M. Matsuda, K. M. Kojima, Y. J. Uemura, J. L. Zarestky, K. Nakajima, K. Kakurai, T. Yokoo, S. M. Shapiro, and G. Shirane, Phys. Rev. B **57**, 11 467 (1998).
[42] M. Hidaka, M. Hatae, I. Yamada, M. Nishi, and J. Akimitsuu, J. Phys.: Condens. Matter **9**, 809 (1997).
[43] S. Egger and I. Affleck, Phys. Rev. B **46**, 10 866 (1992); S. Egger, and I. Affleck, Phys. Rev. Lett. **75**, 934 (1995).
[44] M. Takigawa, N. Motoyama, H. Eisaki, and S. Uchida, Phys. Rev. B **55**, 14 129 (1997).
[45] L. S. Dent-Glasser, Z. Kristallogr. **149**, 291 (1979).